Global Journal of Chemistry, Biology and Physics
Volume 10, Number 4; July-August, 2025;
ISSN: 2836- 8207| Impact Factor: 7.61
https://zapjournals.com/Journals/index.php/GJCBP
Published By: Zendo Academic Publishing

DIVULGING THE COMBINED EFFECTS OF RADIATION, PERTURBATIONS, AND MASS VARIATIONS ON MOTION AROUND AXIAL EQUILIBRIUM POINTS OF THE ROBE'S R3BP

[1]Oni Leke, [1*]Kwaghnzua Barnabas, and [1]Ashezua Timothy
Phone: +2349034443303/ +2347038926452/ +2347032230542
[*]Corresponding Author: bkwaghnzua@gmail.com

Article Info
Keywords: Motion; Axial Equilibrium Points; Earth-Moon System; Artificial Satellite
DOI
10.5281/zenodo.16270238

Abstract
This paper discloses the combined effects of radiation, perturbations, and mass variations on the motion of an artificial satellite around the axial equilibrium points (AEPs) of the Robe's circular restricted three-body problem (RCR3BP). The set-up is such that the masses of the primaries vary with time in accordance with the unified Mestschersky law, and their motion is governed by the Gylden-Mestschersky equation with the further assumption that the second primary (Moon) is a source of radiation and that small perturbations in the Coriolis and centrifugal forces are effective. The non-autonomous dynamical equations are deduced and transformed into the autonomized forms under the condition that the first primary contains no fluid. We investigate the axial equilibrium points and find that the variable mass parameter affects the points due to the centrifugal perturbation and consequently yields finitely many AEPs inside the first primary. These points collinear with the center of the first primary and are defined by the mass parameter, centrifugal force perturbation, radiation pressure factor of the second primary, and variable mass parameter. We also investigated the stability and found that the axial equilibrium points are stable. We applied the study to the motion of an artificial satellite in gravitational environment of the Earth and a radiating Moon. It is seen that the AEP are unstable numerically. Further, we explore the zero-velocity curves of the satellite around the AEPs and observe that the motion of the satellite is possible inside the Earth's sphere in some range of the variable mass parameter but is restricted when the mass gain is high.

[1] Department of Mathematics, College of Physical Science, Joseph Sarwuan Tarka, University, P.M.B. 2373, Makurdi, Benue State, Nigeria

1.0 INTRODUCTION

The restricted three-body problem (R3BP) is a mathematical formulation that studies the motion of an infinitesimal mass, called primaries, which moves and passively gravitates under the attraction of two massive bodies.. The R3BP is of great theoretical, practical, historical, and educational relevance, and in its many variants, has had important implications in several scientific fields, including among others; celestial mechanics, galactic dynamics, chaos theory, and molecular physics. There are many examples of the restricted problem in space dynamics. One of them is the classical three-body problem viz; the Sun-Earth-Moon combination, which describes the motion of the moon. The creation of artificial bodies, which are required to move in the neighborhood of two natural celestial bodies, is one of the foremost in space science. This problem is also similar to the restricted model. The R3BP remains a stimulating and active research area that has attracted the attention of scientists and astronomers because of its applications to the motion of spacecraft and satellites.

A different formulation of the R3BP was developed by Robe (1977). This problem was later called the Robe's Restricted Three Body Problem (RR3BP). A plethora of studies in the RR3BP framework have been explored by various researchers under different modifications and extensions. Amongst these are; Shrivastava and Garain (1991), Plastino and Plastino (1995), Hallan and Rana (2001), Singh and Sandah (2012), Singh and Laraba (2012), Singh and Leke (2013b, c, d), Singh and Omale (2014), Ansari *et al.* (2019) , Abouelmagd et *al*. (2020) , Kaur *et al.* (2020), Kaur and Kumar (2021), Ansari (2021), Kaur et al. (2022). Leke and Ahile (2022) carried out a study on equilibrium points and stability of Robe R3BP with density variation. The equations of motion were deduced, and the equilibrium points and found axial equilibrium point at the center and axial equilibrium points near the center of the first primary. The axial points near the center were further explored, and five types of axial equilibrium points namely; minimal axial points, primary axial points of the first kind, interior points, primary axial points of the second kind, and the terminal point, exists. These points are located either inside the first primary or on the points at which the circle bounding the first primary is coincident with the $x-$axis. Furthermore, a pair of non-collinear and circular equilibrium points, which are points on the circle bounding the first primary, were established. The linear stability of these equilibrium points is investigated, and the axial points at the center and those near the center are conditionally stable analytically but our numerical explorations of the stability reveal that these points can be unstable and stable, a condition that depends on the mass parameter and the density variation of the fluid. The circular points are unstable due to the double roots of the characteristic equation, while the non-collinear equilibrium points are also unstable due to a positive root, which induces instability at the non-collinear equilibrium points. They illustrated the problem numerically for a Submarine-Earth and Moon system and the general case for all mass ratios.

Next, the classical R3BP assumes that the masses of celestial bodies are constant. However, the phenomenon of isotropic radiation or absorption in stars led scientists to deduce the restricted problem of three bodies with variable mass. During evolution, the masses of celestial bodies change, especially in a double-star system, where masses change rather intensively. As an example, we could mention the motion of rockets, formation of black holes, motion of a satellite around a radiating star surrounded by a cloud and varying its mass due to particles of the cloud, and comets loosing part or all of their mass as a result of roaming around the Sun (or other stars) due to their interaction with the solar wind which blows off particles from their surfaces. The motion problem of astronomical objects with variable mass has many interesting applications in stellar, galactic, and planetary dynamics.

The problem of two bodies with variable masses came into science practically following the work of Gylden (1884), who for the relative motion of one mass point about the other mass point under the action of mutual

gravitational force represented the sum of the masses of these points as varying with time by a certain law $m_1 + m_2 = \mu(t)$. Soon afterward, several researchers have relentlessly explored the dynamics of the restricted problem with variable masses. They include Bekov (1988), Luk'yanov (1989), Singh and Leke (2010, 2012, 2013a), Ansari and Sahdev (2022), Leke and Mmaju (2023), Leke and Singh (2023), Putra et al. (2024). Recently, Leke and Orum (2024) and Leke et al (2024, 2025) studied the motion and zero-velocity surfaces around the collinear, triangular, and out-of-plane equilibrium points of the R3BP with a triaxial primary and variable masses, respectively.

The Robe (1977) and its various extensions to problems with constant masses may not be well suited to discuss the dynamics of a test particle when mass variations of the bodies occur. One reason for this is that in problems with constant masses when the shell is empty, there exists one equilibrium point (Robe 1977, Shrivastava and Garain 1991). However, in the context of the RR3BP with variable masses, there is the existence of non-collinear equilibrium points (Singh and Leke 2013b, c). Hence, it is justifiable to explore effects of additional perturbations due to radiation, Coriolis, and centrifugal forces in the RR3BP with variable masses.

2. DYNAMICAL EQUATIONS

Let m_1 be the mass of the first primary fluid, which is a rigid spherical shell of constant radius $\Re$ with center at M_1 , and filled with a homogenous incompressible fluid of constant mass m_f, density δ_1 and volume V_f. Moreover, let m_2 be the mass of the second primary with center at M_2 . Both masses are assumed to vary with time because of the attachment or separation of particles to or from them. We assume that the variation in mass of the first primary occurs isotropically and does not affect the fluid inside it because of the rigid shell. Furthermore, we let m_3 be the mass of the third body with center at M_3, having density δ_3 and its motion is confined inside the spherical shell. Consequently, following Leke and Clement (2024a) and knowing that the distances between the centers of the primaries vary with time; then, the forces acting on m_3 are

i. The attraction force of the radiating second primary is given by

$$\vec{F}_{m_2} = -\frac{Gm_2 q_2 m_3 \bar{r}_{23}}{r_{23}^3} \tag{1}$$

ii. The gravitational force $\vec{F}_A$ exerted by the fluid

$$\vec{F}_A = -\frac{4\pi G \Re^3 m_3 \delta_1 \vec{r}_{13}}{3r_{13}^3} \tag{2}$$

iii. The buoyancy force is given by

$$\vec{F}_B = \frac{4G\pi\Re^3 m_3}{3r_{13}^3}\frac{\delta_1^2 \vec{r}_{13}}{\delta_3} \tag{3}$$

iv. Radiation pressure q_2 of the smaller primary

Where $\vec{r}_{13} = \overrightarrow{M_1 M_3}$ and $\vec{r}_{23} = \overrightarrow{M_2 M_3}$ are the position vectors of the line joining the centers of the first and second primary and the center of the third body, respectively. G is the gravitational constant.

The equation of motion of the third body in the inertial system, considering the forces acting on it, is as follows:

$$\ddot{\vec{R}} = \frac{Gm_2 \vec{r}_{23}}{r_{23}^3} - \frac{4\pi\Re^3}{3}\frac{G\delta_1}{r_{13}^3}\left(1 - \frac{\delta_1}{\delta_3}\right)\vec{r}_{13} \tag{4}$$

Where $\vec{R}=\overrightarrow{OM_3}$, and q_2 is the radiation pressure factors of the smaller primary.

In a synodic coordinates system $Oxyz$ rotating with angular velocity $\vec{\omega}$ and origin at the center of mass, O, of the primaries; the equation of motion (4) is as follows:

$$\frac{\partial^2\vec{R}}{\partial t^2}+2\vec{\omega}\times\frac{\partial\vec{r}}{\partial t}+\vec{R}\times\frac{\partial\vec{\omega}}{\partial t}+\vec{\omega}\times\left(\vec{\omega}\times\vec{R}\right)=-\frac{4\pi\Re^3}{3}\frac{G\delta_1}{r_{13}^3}\left(1-\frac{\delta_1}{\delta_3}\right)\left(x-x_1\right)-\frac{Gm_2q_2\left(x-x_2\right)}{r_{23}^3} \quad (5)$$

Where $\vec{R}$ is the position vector of the third body relative to the center of mass O, and $\vec{\omega}=\omega\hat{k}:\hat{k}$ is a unit vector.

Therefore, the equations of motion of the third body under the set-up of the Robe's CR3BP with variable masses in a Cartesian coordinate system, when the second primary is a radiation source, take the following form:

$$\begin{aligned}
\ddot{x}-2\omega\dot{y}&=\omega^2x+\dot{\omega}y-\frac{4\pi\Re^3}{3}\frac{G\delta_1}{r_{13}^3}\left(1-\frac{\delta_1}{\delta_3}\right)\left(x-x_1\right)-\frac{\mu_2q_2\left(x-x_2\right)}{r_{23}^3}\\
\ddot{y}+2\omega\dot{x}&=\omega^2y-\dot{\omega}x-\frac{4\pi\Re^3}{3}\frac{G\delta_1y}{r_{13}^3}\left(1-\frac{\delta_1}{\delta_3}\right)-\frac{\mu_2q_2y}{r_{23}^3} \quad (6)\\
\ddot{z}&=-\frac{4\pi\Re^3}{3}\frac{G\delta_1z}{r_{13}^3}\left(1-\frac{\delta_1}{\delta_3}\right)-\frac{\mu_2q_2z}{r_{23}^3}
\end{aligned}$$

Where $\mu(t)=\mu_1(t)+\mu_2(t):\ \mu_1(t)=Gm_1,\ \mu_2(t)=Gm_2(t)$

Next, we introduce in equations (6) small perturbations in the Coriolis and centrifugal forces using the parameters, φ and ψ, respectively, to obtain the following equations:

$$\begin{aligned}
\ddot{x}-2\omega\varphi\dot{y}&=\omega^2\psi x+\dot{\omega}\varphi y-\frac{4\pi\Re^3}{3}\frac{G\delta_1}{r_{13}^3}\left(1-\frac{\delta_1}{\delta_3}\right)\left(x-x_1\right)-\frac{\mu_2q_2\left(x-x_2\right)}{r_{23}^3}\\
\ddot{y}+2\omega\varphi\dot{x}&=\omega^2\psi y-\dot{\omega}\varphi x-\frac{4\pi\Re^3}{3}\frac{G\delta_1y}{r_{13}^3}\left(1-\frac{\delta_1}{\delta_3}\right)-\frac{\mu_2q_2y}{r_{23}^3} \quad (7)\\
\ddot{z}&=-\frac{4\pi\Re^3}{3}\frac{G\delta_1z}{r_{13}^3}\left(1-\frac{\delta_1}{\delta_3}\right)-\frac{\mu_2q_2z}{r_{23}^3}
\end{aligned}$$

The over-dot denotes differentiation with respect to time t. φ and ψ are the small perturbations in the Coriolis and centrifugal forces, respectively, such that $\varphi=1+\in$ and $\psi=1+\in':\in<<1$ and $\in'<<1$. While the coordinates (x,y,z) of the third body and ω is the angular velocity of the primaries' revolution.

The equations of motion (7) are non-integrable differential equations with variable coefficients, the solutions even for particular steady-state solutions –the EPs are difficult to obtain directly from equation (7) because they contain unknown functions of time.

Next, following the methodology of Singh and Leke (2013b), we obtain the following autonomized system:

$$\xi''-2\varphi\eta'=\frac{\partial\Omega}{\partial\xi},\ \eta''+2\varphi\xi'=\frac{\partial\Omega}{\partial\eta},\ \zeta''=\frac{\partial\Omega}{\partial\zeta} \quad (8)$$

Where

$$\Omega=\frac{\kappa\psi\left(\xi^2+\eta^2\right)}{2}+\frac{(\kappa-1)\zeta^2}{2}\xi+\frac{\kappa\upsilon q_2}{\rho_{23}} \quad (9)$$

$$\rho_{23}^2=(\xi+\upsilon-1)^2+\eta^2+\zeta^2 \quad (10)$$

Where υ is the mass parameter and is such that $0<\upsilon<1$, while κ is the constant of the particular integral of the GMP.

Equation (8) admits the Jacobian integral

$$2\Omega(\xi,\eta,\zeta)=\left(\xi'^2+\eta'^2+\zeta'^2\right)+C \tag{11}$$

3 LOCATIONS OF THE AXIAL EQUILIBRIUM POINTS

The positions of the AEPs are found by solving the equations $\Omega_\xi=\Omega_\eta=\Omega_\zeta=0$. That is, we need to solve the system of equations

$$(\psi-1)\xi+k\left[\xi-\frac{q_2\upsilon(\xi+\upsilon-1)}{\left[(\xi+\upsilon-1)^2+\eta^2+\zeta^2\right]^{\frac{3}{2}}}\right]=0$$

$$\eta\left\{(\psi-1)+k\left[1-\frac{q_2\upsilon}{\left[(\xi+\upsilon-1)^2+\eta^2+\zeta^2\right]^{\frac{3}{2}}}\right]\right\}=0 \tag{12}$$

$$\zeta\left\{(k-1)-\frac{q_2\kappa\upsilon}{\left[(\xi+\upsilon-1)^2+\eta^2+\zeta^2\right]^{\frac{3}{2}}}\right\}=0$$

3.1 Axial equilibrium point at origin

This equilibrium point was not investigated in previous works by Robe (1977), Shrivastava and Garain (1991), Hallan and Rana (2002), Singh and Leke (2013), and Leke and Clement (2024a, b). They are obtained when we assume that $q_2=0$ in equation (12) to obtain

$$(\psi-1+k)\xi=0 \text{ and } \eta(\psi-1+k)=0 \tag{13}$$

Hence

$$\xi=0,\ \eta=0 \text{ and } (\psi-1+k)\neq 0 \tag{14}$$

which is an equilibrium point at the primaries' origin or center.

If $\psi-1+k=0$ then, $\xi\neq 0,\ \eta\neq 0$

That is, an equilibrium point exists

$$\xi=a,\ \eta=b \tag{15}$$

provided $k=1-\psi$

3.2 The axial equilibrium point near the center

The AEPs near the center are the solutions of equations (12) when $\eta=\zeta=0$. These points lie only on the $\xi-$ plane of motion. Consequently, equation (12) is reduced to the following equation

$$(\psi+k-1)\xi-\frac{q_2k\upsilon(\xi+\upsilon-1)}{(\xi+\upsilon-1)^3}=0 \tag{16}$$

Using the perturbation method, we assume that the solution of Eq. (16) is

$$\xi=-\upsilon+\chi \tag{17}$$

where $\chi<<1$ and $\psi-1<<1$

Substituting (17) in (16) gives

$$-\upsilon(\psi+k-1)+k\chi+\chi(\psi-1)+\frac{q_2k\upsilon}{(1-\chi)^2}=0 \tag{18}$$

Using binomial and ignoring the second and higher powers of χ , and product of $\psi-1$and χ in (18), we obtain the following:

$$\chi = \frac{\upsilon(\psi - 1)}{k(1+2\upsilon)} + \frac{\upsilon(1-q_2)}{1+2\upsilon} \quad (19)$$

where $0 < k < \infty$

Substitute equation (19) in (17), we have

$$\xi = -\upsilon\left[1 - \frac{(\psi - 1)}{k(1+2\upsilon)} - \frac{(1-q_2)}{1+2\upsilon}\right] \quad (20)$$

This gives another equilibrium point on the line joining the centers of the primaries away from the center of the first primary but inside it. Equation (20) is defined by the mass parameter, radiation factor of the second primary, small perturbation in the centrifugal force and the parameter k which describes the primaries' mass variations. The inclusion of the mass variable parameter in (20) leads to the existence of finitely many AEPs near the center of the shell.

When $\kappa = 1$ and the second primary is not a radiation source, we obtain the following:

$\xi = -\upsilon + \frac{\upsilon(\psi - 1)}{(1+2\upsilon)}$ and fully coincides with that of Shrivastava and Garain (1991) and Hallan and Rana (2001).

However, if in equation (20), there is no small perturbation in the centrifugal force, the only equilibrium point reduces to

. $$\xi = -\upsilon\left[1 - \frac{(1-q_2)}{1+2\upsilon}\right] \quad (21)$$

Equation (21) clearly shows the effect of the radiation pressure of the second primary on the location of the axial point lying on the line joining the centers of the primaries and fully coincides with that in Leke and Clement (2024a). When there is no radiation from the second primary, the point fully coincides with that in Robe (1977) and Singh and Leke (2013b). This means that the inclusion of small perturbations in the Coriolis and centrifugal forces admits the existence of the mass variation parameter in the AEP location, which now yields finitely many AEPs

Next, we numerically explore the locations of the AEPs by considering the motion of the Earth's artificial satellites in the gravitational field of the Earth and the Moon. In this premise, we have $\upsilon = 0.01$, $\in = \phi - 1 = 0.003$, $\in' = \psi - 1 = 0.002$, $q_2 = 0.99996$ and $0 < \kappa < \infty$

The AEPs were obtained in equation (20) and defined by the radiationof the smaller primary, small centrifugal force perturbations, and mass variation constant. In Table 1, we numerically compute the axial location of a satellite in the Earth-Moon system.

Table 1: AEPs of a Satellite in the Earth-Moon System for $q_2 = 0.99996$ and $0 < \kappa < \infty$ when $\psi = 1.002$ and $\psi = 1$

κ	$\xi(\psi = 1.002)$	$-2\upsilon \le \xi < 0$	**Remarks**	$\xi(\psi = 1.)$	$-2\upsilon \le \xi < 0$	**Remarks**
0.000000001	19607.8000	NO	Not An EP	-0.01	YES	An EP
0.00001	1.95078000	NO	Not An EP	-0.01	YES	An EP
0.0001	0.18607800	NO	Not An EP	-0.01	YES	An EP
0.001	0.00960785	NO	Not An EP	-0.01	YES	An EP
0.01	-0.00803921	YES	An EP	-0.01	YES	An EP
0.1	-0.00980392	YES	An EP	-0.01	YES	An EP
0.5	-0.00996078	YES	An EP	-0.01	YES	An EP
1	-0.00998039	YES	An EP	-0.01	YES	An EP

2	-0.00999019	YES	An EP	-0.01	YES	An EP
10	-0.00999804	YES	An EP	-0.01	YES	An EP
100	-0.00999980	YES	An EP	-0.01	YES	An EP
1000	-0.00999998	YES	An EP	-0.01	YES	An EP
10000	-0.00999999	YES	An EP	-0.01	YES	An EP
100000	-0.01	YES	An EP	-0.01	Yes	An EP
1000000	-0.01	YES	An EP	-0.01	YES	An EP
$\kappa \to \infty$	-0.01	YES	An EP	-0.01	YES	An EP

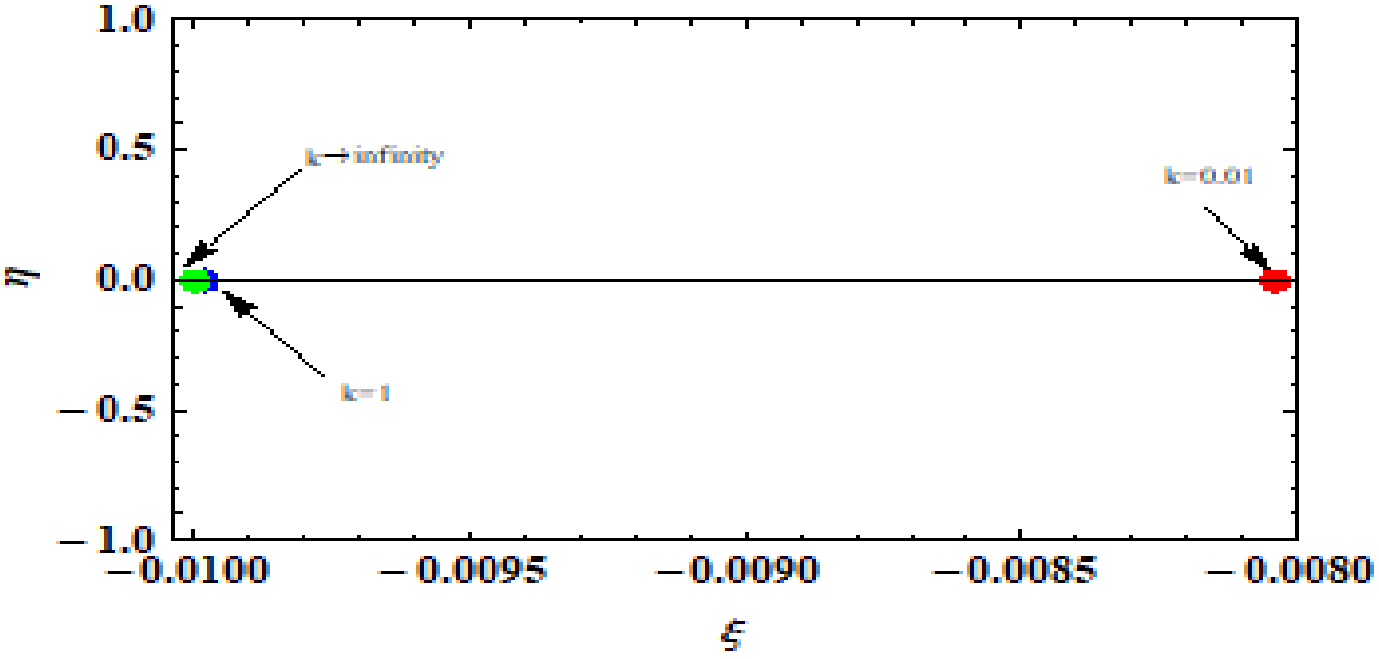

Figure 1: Satellite locations at the AEPs in the Earth-Moon system, for $\kappa = 0.01$ (Red), $\kappa = 1$ (Blue) and $\kappa \to \infty$ (Green)

3.3 Zero-velocity curves around the axial equilibrium points

The Jacobi integral is given in equation (11), where $V = \sqrt{\xi'^2 + \eta'^2 + \zeta'^2}$ is the motion velocity of the satellite and $C$is the Jacobi constant. The allowed motion region and forbidden region of the satellite are defined by $V \geq 0$ and $V < 0$, respectively. Therefore, when the velocity of the satellite is zero, the curve shown by the above equation is called the zero-velocity curve (ZVC) on the plane. ZVCs are important because they form the boundary of regions from which the satellite is dynamically excluded. The regions from which the motion of the satellite is forbidden grow in area as the energy constant increases, and vice versa.

In this section, we explore the ZVC of the Earth's artificial satellite around the AEPs under effects of radiation of the Moon, centrifugal perturbation, and mass variation in the Earth-Moon system. Figure 2 shows the ZVC of the Earth's artificial satellite around the AEPs. The blue region is the region where the motion of the satellite is permissible, whilethe red area is the region where the motion of the satellite is prohibited. The brown spot is the location of the AEPs, and the yellow sphere is the Moon.

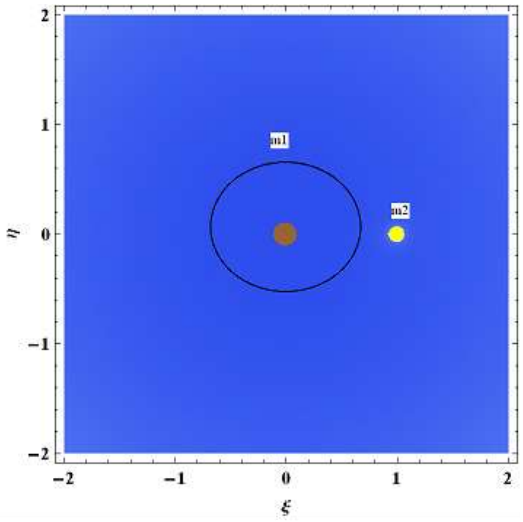

(i).

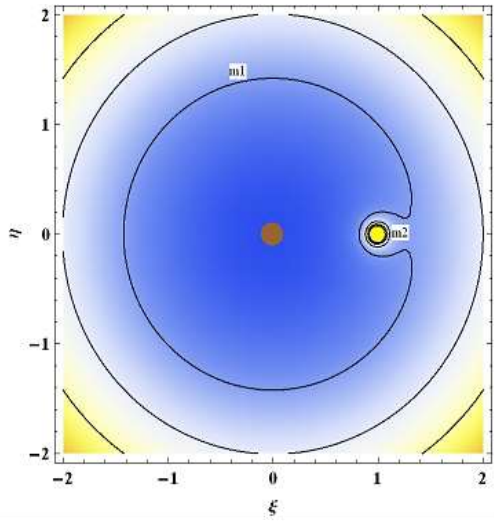

(ii)

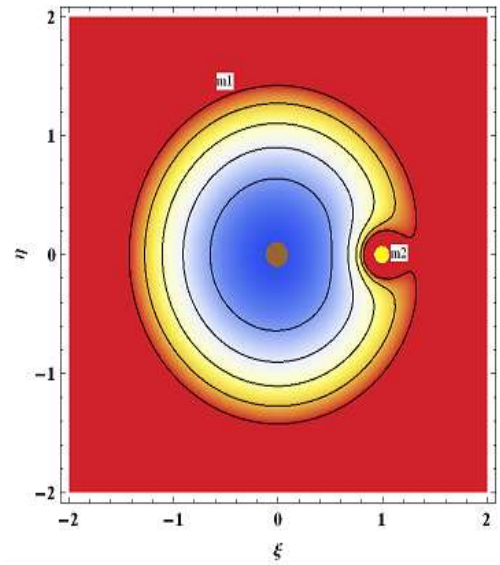

(iii)

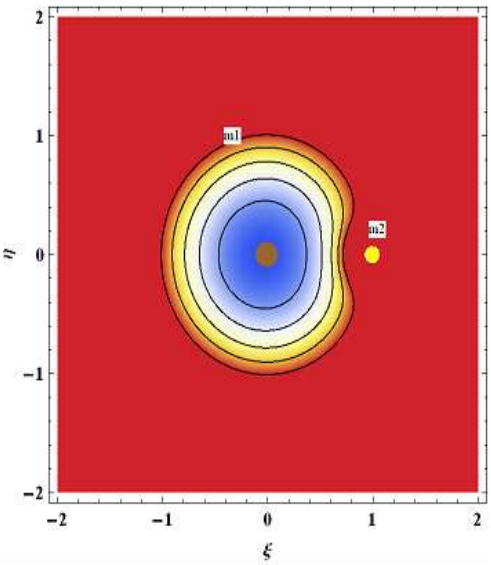

(iv)

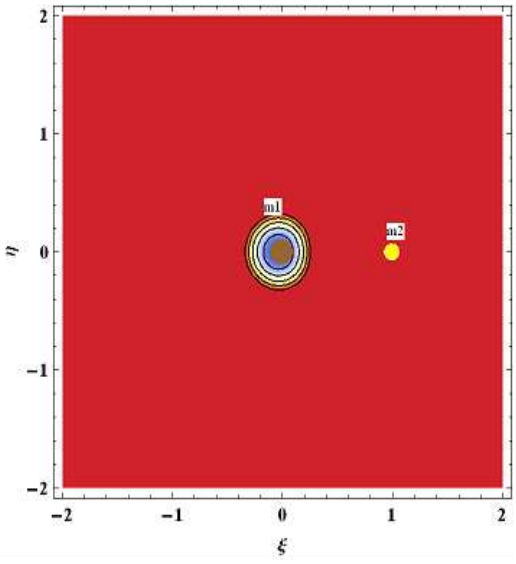

(v)

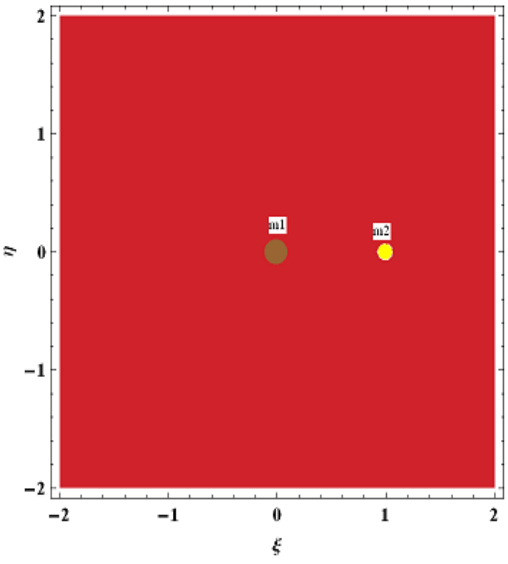

(vi)

Figure 2: ZVC of a Satellite around the AEPs in the Earth-Moon System for $q_2 = 0.99996$, $\psi = 1.002$ and (i) $\kappa = 0.01$ & $C = 0.000402205$ (ii) $\kappa = 0.1$ and $C = 0.00401104$ (iii) $\kappa = 0.5$ and $C = 0.0200505$ (iv) $\kappa = 1$ and $C = 0.0400998$ (v) $\kappa = 2$ and $C = 0.400987$ (vi) $\kappa = 100000$ and $C = 4009.86$

It is seen that as the variable mass parameter increases, there's a corresponding increase in the energy constant, and the blue region diminishes and vanishes as a result. In addition, in Fig. 2i, the satellite is free to move around the AEPs inside the Earth but cannot move around the Moon because its motion is confined within the Earth's sphere. The same analogy follows in Fig. 2ii. In Fig. 2iii-2v, the satellite can travel, but the allowed areas of movement keep shrinking due to the variable mass parameter effect. In Fig. 2vi, the Earth vanishes such that the core located in the forbidden zone remains.

4. STABILITY OF THE AXIAL EQUILIBRIUM POINT

To study the stability of the AEPs located near the center of the empty spherical shell, we apply small displacement *u* and *v* to the coordinates (ξ_0, η_0) of the satellite and to the positions, $\xi = \xi_0 + u$ and $\eta = \eta_0 + v$. If the satellite departs from the vicinity of the point, such a position is unstable. However, if it oscillates about the point, it is in a stable position.

Next, we obtain the following variational equations:

$$u'' - 2\phi v' = \left(\Omega^0_{\xi\xi}\right)u + \left(\Omega^0_{\xi\eta}\right)v$$
$$v'' + 2\phi u' = \left(\Omega^0_{\xi\eta}\right)u + \left(\Omega^0_{\eta\eta}\right)v \qquad (22)$$

The superscript 0 indicates that the partial derivatives are to be evaluated at the equilibrium points.

The characteristic equation corresponding to equations (22) is given as follows:

$$\lambda^4 - \left(\Omega^0_{\xi\xi} + \Omega^0_{\eta\eta} - 4\varphi^2\right)\lambda^2 + \Omega^0_{\xi\xi}\Omega^0_{\eta\eta} - \left(\Omega^0_{\xi\eta}\right)^2 = 0 \qquad (23)$$

where

$$\Omega^0_{\xi\xi} = \psi + \kappa - 1 + 2\kappa\upsilon\left[1 + 3p - (1 - q_2)\right]$$
$$\Omega^0_{\eta\eta} = \psi + \kappa - 1 - \kappa\upsilon\left[1 + 3p - (1 - q_2)\right] \qquad (24)$$
$$\Omega^0_{\zeta\zeta} = \kappa - 1 - \kappa\upsilon\left[1 + 3p - (1 - q_2)\right],\ \Omega^0_{\xi\zeta} = \Omega^0_{\eta\zeta} = \Omega^0_{\xi\eta} = 0$$
$$p = \frac{\upsilon(\psi - 1) + \kappa\upsilon(1 - q_2)}{k(1 + 2\upsilon)},\ p << 1$$

These are the partial derivatives computed at the AEPs (20). When, $\psi = q_2 = 1$ these partial derivatives are fully reduced to those calculated in Singh and Leke (2013b). Furthermore, when $q_2 = \kappa = 1$, the partial derivatives fully coincide with those of Hallan and Rana (2001a) and reduce to that in Robe (1977) when $\psi = q_2 = \kappa = 1$.

After expressing, the characteristic equation (23) after expressing $\varphi = 1 + \in$, is cast to the following forms:

$$\lambda^4 + P\lambda^2 + Q = 0 \qquad (25)$$

where

$$P = 4 + 8 \in -\kappa(2 + \upsilon) - 2 \in' -3p\kappa\upsilon + \kappa\upsilon(1 - q_2)$$
$$Q = \kappa^2\left[\left(1 + \upsilon - 2\upsilon^2\right) + p\upsilon(3 - 12\upsilon) - \upsilon(1 - 4\upsilon)(1 - q_2) + \frac{(2 + \upsilon)\in'}{\kappa}\right]$$

Evidently, $Q>0$, while $P <=> 0$ when $\kappa <=> \frac{4+8\in -2\in'}{\left[2+\upsilon+3p\upsilon-\upsilon(1-q_2)\right]}$, respectively.

The roots are

$$\lambda_{1,2}^2=\frac{-\left[4+8\in-\kappa(2+\upsilon)-2\in'-3p\kappa\upsilon+\kappa\upsilon(1-q_2)\right]\pm\sqrt{D}}{2} \quad (26)$$

where

$$D=-16(\kappa-1)+\kappa\upsilon(9\kappa\upsilon-8)+16(4-2\kappa-\kappa\upsilon)\in-16\in'-6p\kappa\upsilon(4-9\kappa\upsilon)+2\kappa\upsilon(4-9\kappa\upsilon)(1-q_2)(27)$$

When there are no perturbations in the Coriolis and centrifugal forces and the second primary is not a radiation source, we have the following:

$$D=-16(\kappa-1)+\kappa\upsilon(9\kappa\upsilon-8) \quad (28)$$

This coincides with the results obtained by Singh and Leke (2013b)

Now, using the equation

$$\upsilon=\frac{-b\pm\sqrt{b^2-4ac}}{2a}$$

We solve equation (27) for υ when the discriminant vanishes to obtain the critical mass parameter given by

$$\upsilon_{C\kappa}=\frac{4}{9\kappa}\left[1+\sqrt{(9\kappa-8)}\sqrt{1+2(1-q_2)}+(1-q_2)+\frac{\left(27\kappa^2-120\kappa+132-48\kappa\sqrt{(9\kappa-8)}+54\sqrt{(9\kappa-8)}\right)\in'}{2\kappa\sqrt{9\kappa-8}}\right.$$

$$\left.\frac{\left(9\kappa-16+2\sqrt{(9\kappa-8)}\right)\in}{\sqrt{9\kappa-8}}\right] \quad (29)$$

Equation (29) is the values of the critical mass parameter which exists for different values of the variable mass parameter, small perturbations in the Coriolis and centrifugal forces, and Moon radiation. When there are no perturbations in the Coriolis and centrifugal forces, that is $\in=\in'=0$ and when the second primary is not a source of radiation, that is $q_2=1$, the critical mass reduces to that in Singh and Leke (2013b). Furthermore, when $\kappa=1$ (that is when mass variations are ignored), the critical mass reduces to that obtained by Robe (1977) and Hallan and Rana (2001a).The critical mass values exist for $\kappa\geq\frac{8}{9}$.

Since the nature of the roots depends on the discriminant, mass ratio, and mass variable constant; we consider the three regions of equation (27) coupled with the changes in the coefficient of λ^2.

1. When simultaneously, $\kappa>\frac{4+8\in-2\in'}{\left[2+\upsilon+3p\upsilon-\upsilon(1-q_2)\right]}$ or $\kappa<\frac{4+8\in-2\in'}{\left[2+\upsilon+3p\upsilon-\upsilon(1-q_2)\right]}$ and $0<\upsilon<\upsilon_{c\kappa}$, $D<0$; the roots are complex with real positive parts, rendering the AEPs unstable

2. When $\upsilon=\upsilon_{c\kappa}$, $D=0$; these cases are possible

a. If $\kappa<\frac{4+8\in-2\in'}{\left[2+\upsilon+3p\upsilon-\upsilon(1-q_2)\right]}$ and $0<\upsilon<\upsilon_{c\kappa}$, two roots are real and equal, while the remaining two are negative and equal. The AEP is unstable.

b. If $\kappa=\frac{4+8\in-2\in'}{\left[2+\upsilon+3p\upsilon-\upsilon(1-q_2)\right]}$ and $0<\upsilon<\upsilon_{c\kappa}$, here all the roots are zero and the AEP is unstable.

c. If $\kappa > \frac{4+8\in -2\in'}{\left[2+\upsilon+3p\upsilon-\upsilon(1-q_2)\right]}$ and $0<\upsilon<\upsilon_{c\kappa}$, all the four roots are imaginary with two positive and equal roots and the other two roots are negative and equal roots. In this case, we have a stable positive resonance.

3. When $\upsilon_{c\kappa}<\upsilon<1$, D is positive; here when $\kappa > \frac{4+8\in -2\in'}{\left[2+\upsilon+3p\upsilon-\upsilon(1-q_2)\right]}$ and $0<\upsilon<\upsilon_{c\kappa}$, the roots are all distinct pure imaginary. In this case, the AEP is stable. However, when $\kappa = \frac{4+8\in -2\in'}{\left[2+\upsilon+3p\upsilon-\upsilon(1-q_2)\right]}$, there are two positive and negative equal roots; while for $\kappa < \frac{4+8\in -2\in'}{\left[2+\upsilon+3p\upsilon-\upsilon(1-q_2)\right]}$, the roots are real and distinct. The AEP is unstable in both cases due to a positive root.

Hence, we conclude that the EP is stable for $\upsilon_{c\kappa}<\upsilon<1$ provided $\kappa > \frac{4+8\in -2\in'}{\left[2+\upsilon+3p\upsilon-\upsilon(1-q_2)\right]}$; otherwise, it is unstable.

The nature of the roots of the characteristic equation depends on the discriminant, the radiation pressure of the Moon, small perturbations in the Coriolis and centrifugal forces, mass ratio υ, and the constant κ of mass variation. We shall numerically determine the roots of the characteristic equation and the critical masses in Table 2.

Table 2: Characteristic Roots and the Critical Mass Parameter of the AEPs of a Satellite in the Earth-Moon System for $q_2 = 0.99996$, $\psi = 1.002$ and $0.01<\kappa<\infty$

κ	$\pm\omega_1$	$\pm\omega_2$	$\upsilon_{C\kappa}$
0.01	0.00594118i	1.99997i	Complex
0.1	0.05245520i	1.95352i	Complex
0.5	0.29479400i	1.71117i	Complex
0.8	0.55570800i	1.45024i	Complex
0.88	0.65706600i	1.34888i	Complex
0.89	0.67191000i	1.33403i	0.652914
0.9	0.68745200i	1.31849i	0.570009
0.95	0.78092300i	1.22501i	0.617498
0.995	0.93908100i	1.06685i	0.673890
0.999	0.99511200i	1.01082i	0.678809
1	Complex	Complex	0.680036
2	Complex	Complex	1.330520
3	Complex	Complex	1.553410
5	Complex	Complex	1.732570
10	Complex	Complex	1.867080
100	Complex	Complex	1.987420
1000	Complex	Complex	1.999060
$\kappa\to\infty$	Real	Real	2.000160

5. DISCUSSION

In this paper, the RR3BP in which the masses of the primaries are assumed to vary with time under the additional influence of small perturbations in the Coriolis and centrifugal forces, and the radiation pressure of the smaller primary, has been studied. We found two kinds of AEPs. The first is the one at the origin, which invariably does not lie inside the shell, and the second is the AEPs near the center of the shell obtained in equation (20), and defined by the radiation of the smaller primary, small perturbations in the centrifugal force, and the mass variation constant.

Table 1 shows the locations of the Earth's artificial satellites in the Earth-Moon system under effects of the radiation pressure of the Moon, mass variation constant of the Earth and Moon, in the presence and absence of small centrifugal force perturbations. Table 1 shows that when $0 < \kappa < 0.01$ and $\psi = 1.002$, the points lie outside the Earth's enclosure, and so the AEPs of the satellite do not exist in this interval. However, $0.01 \le \kappa < \infty$ and $\psi = 1.002$ the satellite is located inside the Earth's sphere. Hence, there are finitely many AEPs located inside the Earth on the line joining the Earth and the moon.

Similarly, from Table 1, we computed the AEPs in the absence of a small perturbation in the centrifugal force, that is $\psi = 1$. Only one axial EP exists, which is independent of the mass variation constant of the Earth and Moon.

The graph of AEPs of the satellite in the Earth-Moon gravitational field is drawn in Figure 1 under effects of radiation pressure of the Moon, centrifugal perturbation, and Earth and Moon mass variations. The red point signifies the satellite's position when $\kappa = 0.01$, while the blue and green points indicate the position of the satellite when $\kappa = 1$ and $\kappa \to \infty$, respectively.

In order to discuss, the stability of motion of the satellite around the AEPs we computed in Table 2 the roots of the characteristic equation and the critical mass parameter corresponding to the AEPs under effects of radiation pressure of the Moon, small perturbations in the Coriolis and centrifugal forces, and the mass variation parameter of the Earth and Moon. We computed the roots and critical mass in the AEPs' existence region, that is when $0.01 < \kappa < \infty$. It is seen that when $0.01 < \kappa \le 0.999$, the four roots are pure imaginary roots. However, these roots change to complex roots when $1 \le \kappa < \infty$. When the constant mass variation tends to infinity, the roots become real roots. The numerical estimates of the critical mass parameter have been computed in Table 2 (last column). When the mass variation constant is in the interval $0.01 \le \kappa \le 0.88$, the values of the critical mass are complex and hence do not exist. However, when $0.89 \le \kappa < \infty$ the values are real, the critical mass value should not exceed one because we have $0 < \upsilon < 1$. Therefore, any critical mass value exceeding one is ignored and taken not to exist. Therefore, the critical mass parameter of AEPs exists when $0.89 \le \kappa \le 1$.

Now, in order to analyze the stability of the AEPs, a necessary and sufficient condition for stability of the AEPs is that all four roots are simultaneously pure imaginary roots and $\upsilon_{c\kappa} < \upsilon < 1$. However, only the necessary part is guaranteed in the interval $0.01 < \kappa \le 0.999$ with the sufficient part not fulfilled. Hence, the satellite motion around the AEPs is unstable, in the linear sense.

Next, we explored the ZVC of a satellite around the AEPs (Fig.2) for values of the radiation pressure of the Moon, centrifugal perturbation, and host body mass variations. The blue region depicts the region where the motion of the satellite is permitted, while the red region is the region where the satellite is restricted to travel, Fig 2 depicts the ZVC around AEPs when $\upsilon = 0.01$, under radiation pressure of the Moon. It is seen that for $\kappa = 0.01$ the energy constant is $C = 0.000402205$. In this case, the motion of the satellite is allowed within the

Earth's sphere. Furthermore, when $\kappa = 0.1$ and $\kappa = 0.5$, respectively, the motion satellite around the AEPS inside the Earth's sphere is permitted, but the permitted motion regions shrink with increasing variable mass parameters.

6 CONCLUSION

This paper studied Robe's (1977) R3BP when the masses of the first and second primary vary isotropically with time in accordance with the unified Mestschersky law and their motion described by the Gylden-Mestschersky problem under the effects of small perturbations in the Coriolis and centrifugal forces and radiation pressure of the second primary. The non-autonomous equations of the dynamical system were deduced and transformed to equations of motion with constant coefficients when the fluid densities inside the first primary and the infinitesimal mass density are equal. In other words, the shell is empty. AEPs near the center of the shell exist. These points are defined by the radiation pressure of the second primary, the mass parameter, the small perturbation in the centrifugal force, and the variable mass parameter. The AEPs are numerically unstable for the Earth-Moon system. The zero-velocity curves around the AEPs were explored, and it is seen that under the combined effects of radiation, perturbation, and mass variations, the motion of the Earth's artificial satellite is restricted when the mass gain is very high.

REFERENCES

Abouelmagd, E. I., Ansari, A. A.& Shehata, M. H. (2020). Based on Robe's restricted problem with a modified Newtonian potential. *International Journal of Geometric Methods in Modern Physics, 18*(01): 2150005. doi:10.1016/j.ijgm.2015.09.015

Ansari, A. A., Singh, J., Alhussain, Z. A., & Belmabrouk, H. (2019). Perturbed Robe's CR3BP with viscous force. *Astrophysics and Space Science, 364:*1-7.

Ansari, A. A. (2021). Kind of Robe's restricted problem with heterogeneous irregular primary of N-layers when the outermost layer has viscous fluid. *New Astronomy, 83:* 101496.

Ansari, A. A., & Sahdev, S. K. (2022). Variable Mass Body Motion in the Perturbed Robes Configuration. *Astronomy Reports*, *66*(7): 595-605.

Bekov, A. A.: (1988). Libration Points of the Restricted Problem of Three Bodies with Variable Mass. *Soviet Astronomy Journal,33:* 92-95

Gylden, H.: (1884). Die Bahnbewegungen in Einem Systeme von zwei Körpern in Dem Falle, Dass Die Massen Ver Nderun- Gen Unterworfen Sind, and Astronomische Nachrichten.*109:* 1-6.

Hallan, P.P. and Rana, N. (2001). Existence and Stability of Equilibrium Points in Robe Restricted Three-Body Problem. *Celestial Mechanics and Dynamical Astronomy*, *79:* 145–155.

Kaur, B., Kumar, D., &Chauhan, S. (2020). Effect of Coriolis and centrifugal force perturbations in the Robe-finite straight segment model with arbitrary density parameter. *Astronomische Nachrichten, 341*(1):32-43.

Kaur, B., and Kumar, S. (2021). Stability analysis in the perturbed CRR3BP finite straight segment model under the effect of viscosity. *Astrophysics and Space Science*, *366*(5):43.

Kaur, B., Kumar, S., &Aggarwal, R. (2022). Effects of Viscosity and Oblateness on the Perturbed Robes Problem with Non-Spherical Primaries. *Kinematics and Physics of Celestial Bodies*, *38*(5): 248-261.

Leke, O., & Ahile, G. (2022). A Study on Equilibrium Points and Stability of Robes R3BP with Density Variation. *Journal of Applied Physical Science International*, *14*(3):13-41.

Leke, O., & Singh, J. (2023). Out-of-plane equilibrium points of extra-solar planets in the central binaries PSR B1620-26 and Kepler-16 with clusters of material points and variable masses. *New Astronomy, 99:* 101958.

Leke, Oand Mmaju, C (2023). Zero velocity curves of a dust grain around equilibrium points under effects of radiation, perturbations, and variable Kruger 60.. *Physics. Astronomy. International Journal.* 7, 280-285

Leke, O and Clement M, (2024a). Equilibrium Points and Locations in the Photogravitational Circular Robe's Restricted Three-Body Problem with Variable Masses, DUJOPAS *10,* 188-201

Leke, O and Clement M, (2024b) Effect of Radiation Pressure on Dynamical Structures In the R3BP of Circular Robe with Variable Masses. *FJS 8, 210–223*

Leke, O., & Orum, S. (2024). Motion and zero-velocity curves of a dust grain around collinear libration points for binary IRAS 11472-0800 and G29-38 with a triaxial star and variable masses. *New Astronomy, 108:* 102-177.

Leke, O and Amuda, T.O (2024). Locations of triangular equilibrium points of the Restricted Three-Body Problem with Poynting-Robertson drag and variable masses *FUDMA Journal of Sciences8, 313-318*

Luk'yanov, L. G., (1989). Particular Solutions in the Restricted Problem of Three Bodies with Variable Masses. *Astronomical Journal of Academy of Sciences of USSR, 66:180-187*

Plastino, A. R.,& Plastino, A.: (1995). Robe's Restricted Three-Body Problem Revisited. *Celestial Mechanics and Dynamical Astronomy*, *61:*197–206.

Putra, L.B., Nurul Huda, I., Ramadhan, H. S., et al. 2024. Effects of the variable mass, disk- like structure, and radiation pressure on the dynamics of the circular restricted three- body problem. Romanian Astron. J. Doi: 10.59277/RoAJ.2023.1-2.03

Robe, H, A. G., (1977). A New Kind of Three Body Problem, *Celestial Mechanics*,,1: 343–351.

Shrivastava, A.K. and Garain, D.N.: (1991). Effect of Perturbation on the Location of Libration Point in the Robe Restricted Problem of Three Bodies, *Celestial Mechanics and Dynamical Astronomy*, *51:* 67-73.

Singh, J., & Leke, O., (2010). Stability of the photo gravitational restricted three-body problem with variable masses. Astrophysics and Space Science, 326, 305- 314.

Singh, J. and Leke, O. (2012). Equilibrium points and stability in the restricted three-body problem with oblateness and variable masses. *Astrophysics and Space Science, 340*(1): 27-41.

Singh, J., & Sandah, A.U. (2012). Existence and Linear Stability of Equilibrium Points in the Robe's Restricted Three-Body Problem with Oblateness. *Advances in Mathematical Physics, 2012*, Article ID 679063, 18 pages [Remark 1]

Singh, J., & Laraba, H.M. (2012). Robe's Circular Restricted Three-Body Problem under Oblate and Triaxial Primaries. *Earth Moon and Planets, 109:* 1–11

Singh, J., & Leke, O. (2013a). Effect of oblateness, perturbations, radiation, and varying masses on the stability of equilibrium points in the restricted three-body problem. *Astrophysics and Space Science*, *344:* 51-61.

Singh, J., & Leke, O. (2013b). Existences and Stability of equilibrium point in the robes restricted three body problem with variable masses. *International Journal of astronomy and astrophysics*, 3, 113-122

Singh, J., & Leke, O.: (2013c) "Robe's Restricted Three-Body Problem with Variable

Masses and Perturbing Forces" *ISRN Astronomy* and *Astrophysics,* 2013.*Article ID: 910354*

Singh, J., & Leke, O.: (2013d) "On Robe's Circular Restricted Problem of Three "Variable Mass Bodies," *Journal of Astrophysics.* 2013*, Article ID 898794,*

Singh, J., & Omale, J.A. (2014). Robe's Circular Restricted Three-Body Problem with Zonal Harmonics. *Astrophysics and Space Science,353:* 89-96

Szebehely, V. G. (1967). Stability of the Points of Equilibrium in the Restricted Problem, *Astronomical Journal*, *72:* 7-9.